Available online at www.sciencedirect.com

SciVerse ScienceDirect

Ceramics International 39 (2013) 1335–1340

CERAMICS INTERNATIONAL

www.elsevier.com/locate/ceramint

Dielectric properties and bright red emission of Y^{3+}/Eu^{3+}-codoped ZrO_2 thin films prepared by chemical solution deposition

Lirong Liang, Hong Zhou, Guangheng Wu, Zhong Mo, Dinghua Bao*

State Key Laboratory of Optoelectronic Materials and Technologies, School of Physics and Engineering, Sun Yat-Sen University, Guangzhou 510275, PR China

Received 12 June 2012; received in revised form 12 July 2012; accepted 21 July 2012
Available online 27 July 2012

Abstract

We report on an effective combination of good dielectric properties with bright red emission in Y^{3+}/Eu^{3+}-codoped ZrO_2 thin films. The thin films were deposited on fused silica and $Pt/TiO_2/SiO_2/Si$ substrates using a chemical solution deposition method. The crystal structure, surface morphology, electrical and optical properties of the thin films were investigated in terms of annealing temperature, and Y^{3+}/Eu^{3+} doping content. The $5\%Eu_2O_3$–$3\%Y_2O_3$–$92\%ZrO_2$ thin film with 400 nm thickness annealed at 700 °C exhibits optimal photoluminescent properties and excellent electrical properties. Under excitation by 396 nm light, the thin film on fused silica substrate shows bright red emission bands centered at 593 nm and 609 nm, which can be attributed to the transitions of Eu^{3+} ions. Dielectric constant and dissipation factor of the thin films at 1 kHz are 30 and 0.01, respectively, and the capacitance density is about 65.5 nf/cm^2 when the bias electric field is less than 500 kV/cm. The thin films also exhibit a low leakage current density and a high optical transmittance with a large band gap.

Keywords: C. Electrical property; Y^{3+}/Eu^{3+}-codoped ZrO_2 thin film; Photoluminescence; Chemical solution deposition

1. Introduction

Zirconium oxide (ZrO_2) is one of the widely studied oxide materials over the last two decades because of its excellent electrical and optical properties, such as high dielectric constant (about 23–29), good thermal stability, high melting point, and wide band gap (5–7 eV) [1,2]. It has exhibited some important technological applications in catalyst supports, oxygen detectors, high-temperature fuel cell electrolytes, gate dielectric in metal oxide semiconductor devices, resistive switching memories, and optical waveguides [3,4]. Usually, ZrO_2 has three primary polymorph phases (monoclinic, tetragonal, and cubic) [5]. The phase structure of ZrO_2 significantly influences its physical properties. At room temperature pure ZrO_2 is unstable, properly doping Y_2O_3 into ZrO_2 can form a fully stable phase structure. In previous studies more attention has been paid to 8% Y_2O_3–$92\%ZrO_2$ (YSZ) because of its excellent structural and chemical stability [6–8].

On the other hand, photoluminescent materials have attracted much interest due to the increasing demand for optoelectronic and photonic devices, and biomedical applications [9,10]. Eu-doped ZrO_2 is considered to be an efficient rare earth photoluminescent oxide material [11]. The rare-earth-doped oxide photoluminescent materials exhibit unique optical properties such as high luminescence efficiency and good photochemical stability [12,13].

There has been extensive research on electrical properties of Y-doped ZrO_2 and on photoluminescent properties of Eu-doped ZrO_2. However, little work has been reported on Y/Eu-codoped ZrO_2 thin films [11]. It should be interesting to simultaneously obtain good photoluminescence and electrical properties in Y/Eu-codoped ZrO_2 thin films. In this study, the crystal structure, surface morphology, electrical and optical properties of Y^{3+}/Eu^{3+}-codoped

*Corresponding author. Tel./fax: +86 20 8411 3365.
E-mail address: stsbdh@mail.sysu.edu.cn (D. Bao).

0272-8842/$ - see front matter © 2012 Elsevier Ltd and Techna Group S.r.l. All rights reserved.
http://dx.doi.org/10.1016/j.ceramint.2012.07.069

ZrO_2 thin films were investigated. Our results demonstrated an effective combination of the excellent photoluminescent and electrical properties in Y^{3+}/Eu^{3+}-codoped ZrO_2 thin films.

2. Experimental procedure

The Y^{3+}/Eu^{3+}-codoped ZrO_2 thin films were deposited on fused silica and $Pt/TiO_2/SiO_2/Si$ substrates using a chemical solution deposition method. The precursor solutions were synthesized as follows: firstly, zirconium n-propanol was added to 2-methoxyethanol and glacial acetic acid, a certain amount of acetylacetone was used as the chelating and stabilizing reagent. Then, yttrium acetate and europium nitrate were added to the above solutions. After continuously heating for 10 min and stirring for 3 h, the precursor solutions were obtained with a concentration of 0.3 mol/l. These solutions were spin-coated onto the substrates at a spinning rate of 3000 rpm for 20 s using a commercial spinner. After each coating step, the films obtained were baked at 300 °C for 5 min on a hot plate to remove organics. Then, the spin-coating and baking procedure was repeated until the desired film thickness was attained. The resulting thin films were annealed at different temperatures in air for 1 h.

The crystallization and structure of the thin films were identified using a Rigaku x-ray diffraction (XRD) unit (D/MAX 2200 VPC, Rigaku Corp, Sendagaya, Shibuya-Ku, Tokyo, Japan) with Cu Kα radiation operated at 40 kV and 30 mA. The surface morphologies and thickness of the thin films were examined by scanning electron microscopy (JEOL, JSM-7000 F, JEOL Ltd. Akishima, Tokyo, Japan), and the images were taken at 10 kV. The surface morphologies and surface roughness of the thin films were also observed by an atomic force microscopy (AFM, Veeco Metrology, Santa Barbara, California, USA). To measure the electrical properties, Pt top electrodes were deposited on the surfaces of the thin films through a shadow mask. Dielectric constant and dielectric loss of the thin films were measured using Agilent 4284A LCR meter with applied ac signal amplitude of 100 mV. The leakage current characteristics of the thin films were obtained using Keithley 236 sourcemeter. The UV excitation and emission spectra of the thin films were measured using a Shimadzu RD-5301PC spectrofluorophotometer (Shimadzu Corp, Nakagyo-Ku, Kyoto, Japan). The UV–Vis spectra were recorded with a Shimadzu UV -3150 spectrophotometer in the wavelength range of 200–1500 nm.

3. Results and discussion

Fig. 1 shows the XRD patterns of $3\%Eu_2O_3$–$5\%Y_2O_3$–$92\%ZrO_2$ thin films prepared on $Pt/TiO_2/SiO_2/Si$ substrates, annealed at various temperatures in air for 1 h. It can be noted that the five reflection peaks in the XRD patterns correspond to the (101), (110), (102), (112) and (103), indicating that all the thin films with different Eu contents show tetragonal phases. As the annealing temperature increases, the full width at half maximum of the XRD peaks decreases, indicating the enhanced crystallinity of the thin films.

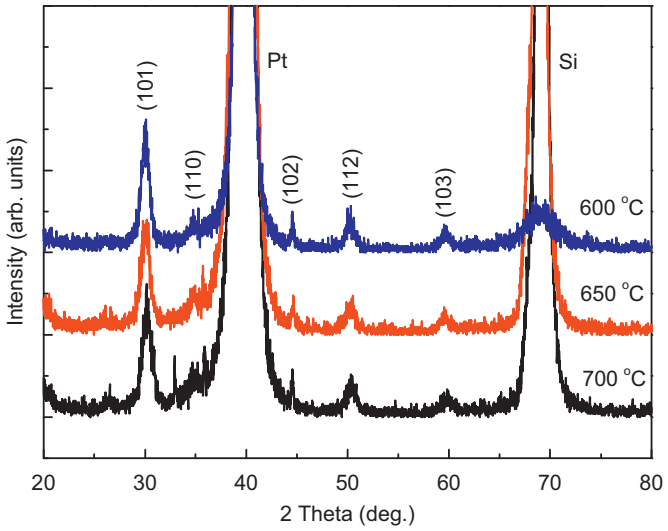

Fig. 1. The XRD patterns of $3\%Eu_2O_3$–$5\%Y_2O_3$–$92\%ZrO_2$ thin films prepared on $Pt/TiO_2/SiO_2/Si$ substrates annealed at various temperatures.

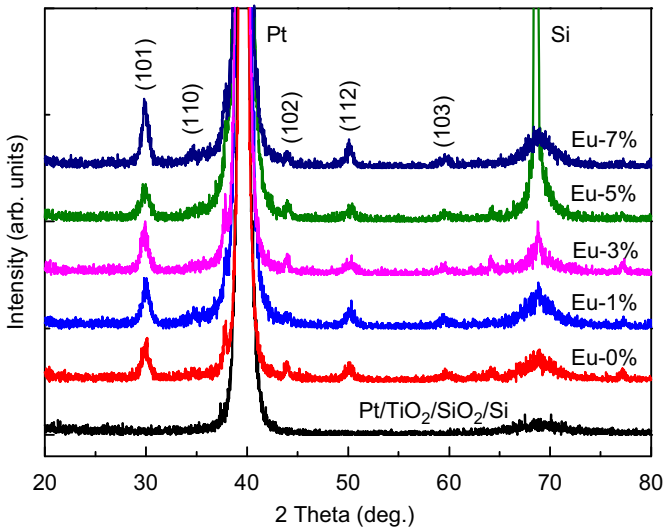

Fig. 2. The XRD patterns of $x\%Eu_2O_3$–$(8-x)\%Y_2O_3$–$92\%ZrO_2$ thin films ($x=0$, 1, 3, 5, and 7, respectively) prepared on $Pt/TiO_2/SiO_2/Si$ substrates annealed at 700 °C in air for 1 h.

Fig. 2 shows the XRD patterns of $x\%Eu_2O_3$–$(8-x)\%Y_2O_3$–$92\%ZrO_2$ thin films ($x=0$, 1, 3, 5, and 7, respectively) prepared on $Pt/TiO_2/SiO_2/Si$ substrates annealed at 700 °C in air for 1 h. It can be seen that the XRD patterns almost remains unchanged, irrespective of Eu concentration. Neither phase transition nor additional impurity phase appear, suggesting that Y/Eu molar ratio has no obvious effect on phase structure of ZrO_2 thin films.

Fig. 3(a) and (b) shows the surface and cross-sectional scanning electron micrographs of the $5\%Eu_2O_3$–$3\%Y_2O_3$–$92\%ZrO_2$ thin film deposited on $Pt/TiO_2/SiO_2/Si$ substrates.

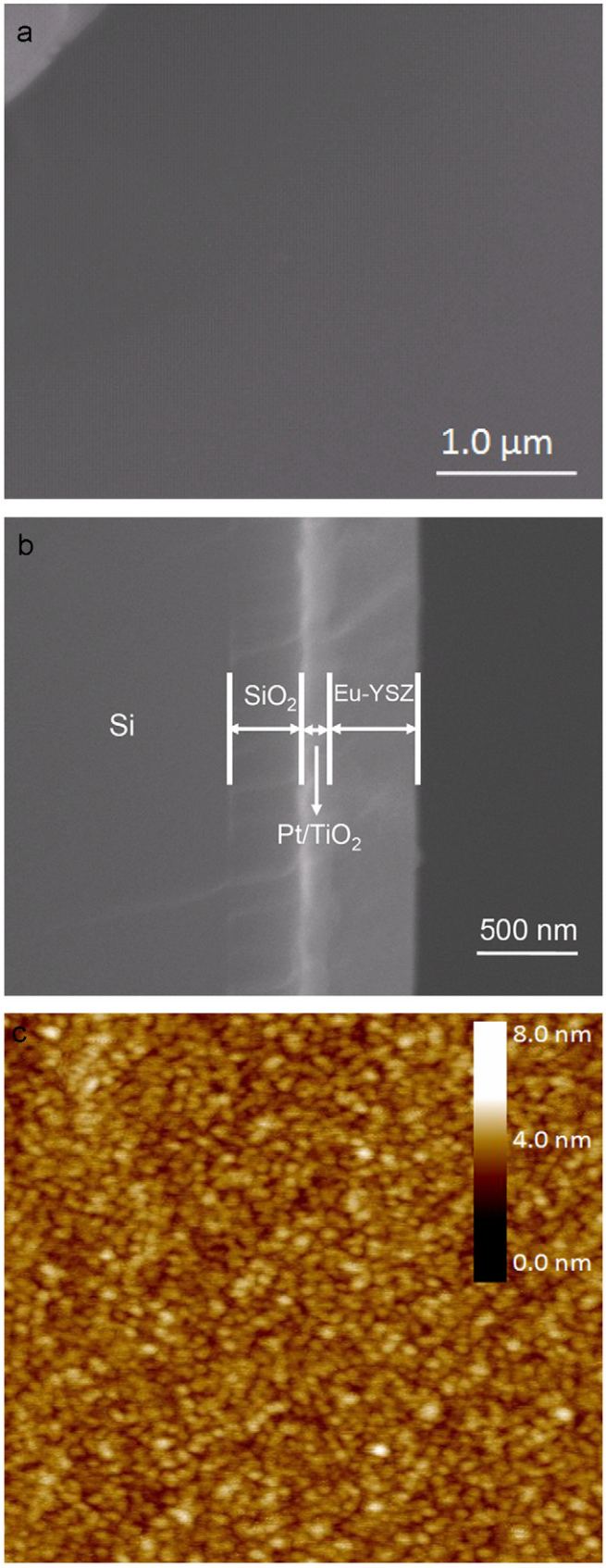

Fig. 3. (a) The surface, (b) cross-sectional scanning electron micrographs, and (c) AFM image (1 μm × 1 μm) of the 5%Eu_2O_3–3%Y_2O_3–92%ZrO_2 thin film deposited on Pt/TiO_2/SiO_2/Si substrate annealed at 700 °C in air for 1 h.

The thin film is smooth and continuous without particles and cracks. It is evident that the thin film exhibits dense microstructure and uniform thickness of approximately 400 nm. In order to clearly observe the surface morphology and surface roughness of the thin film, an AFM with tapping-mode was used. As shown in Fig. 3(c), the root mean square roughness of the 5%Eu_2O_3–3%Y_2O_3–92%ZrO_2 thin film is 0.35 nm.

We have investigated the electrical properties of the thin films, such as dielectric properties, capacitance–voltage (C–V) characteristics and current–voltage (I–V) characteristics of the x%Eu_2O_3–(8-x)%Y_2O_3–92%ZrO_2 thin films (x=0, 1, 3, 5, and 7, respectively), which were prepared on Pt/TiO_2/SiO_2/Si substrates and annealed at 700 °C for 1 h in air. Fig. 4 shows the variation of dielectric constant and dissipation factor with frequency measured at room temperature for the thin films with different europium concentrations. The dielectric constant of the thin films does not change obviously with europium concentration within 1–3%, except for the singly Y^{3+}-doped ZrO_2 thin films. The dissipation factor decreases with increasing europium concentration. Both the dielectric constant and the dissipation factor do not show obvious frequency dispersion in the measured frequency range. The dielectric constant and dissipation factor are about 30 and 0.01 at 1 kHz, respectively, for the 5%Eu_2O_3–3%Y_2O_3–92%ZrO_2 thin film. The dielectric constant is close to that (~27) reported for YSZ films [1,14,15]. But the dissipation factor is much lower than 0.1 reported for YSZ films on Pt/TiO_2/SiO_2/Si substrate [16].

Fig. 5 shows the dependence of the capacitance density of the thin films on the bias electric field measured at a frequency of 1 kHz at room temperature. It can be noted that the capacitance density exhibits little variation with the applied electric field for the thin films with various europium concentrations. The capacitance density is about 65.5 nf/cm^2 at a bias electric field of 500 kV/cm and the dissipation factor obviously decreases with increasing

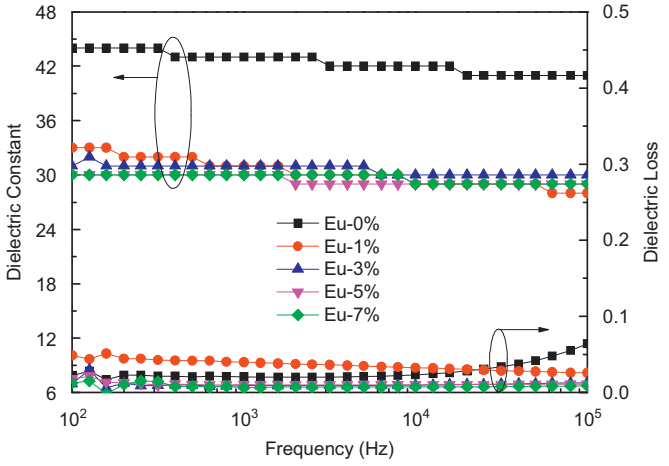

Fig. 4. The variation of dielectric constant and dissipation factor with frequency for the x%Eu_2O_3–(8−x)%Y_2O_3–92%ZrO_2 thin films (x=0, 1, 3, 5, and 7, respectively) prepared on Pt/TiO_2/SiO_2/Si substrates.

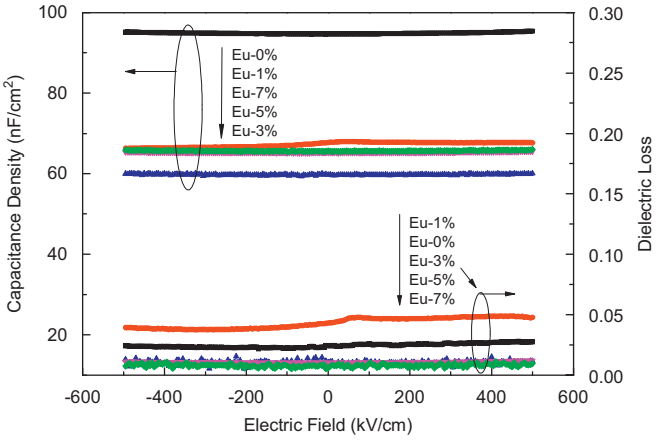

Fig. 5. The dependence of the capacitance density on bias voltage for the $x\%Eu_2O_3$–$(8-x)\%Y_2O_3$–$92\%ZrO_2$ thin films ($x=0$, 1, 3, 5, and 7, respectively) prepared on $Pt/TiO_2/SiO_2/Si$ substrates.

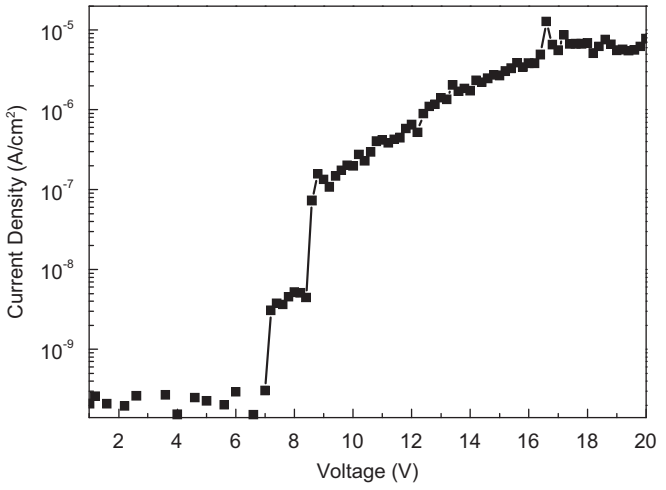

Fig. 6. The leakage current density versus applied bias field for the $5\%Eu_2O_3$–3% Y_2O_3–$92\%ZrO_2$ thin film deposited on $Pt/TiO_2/SiO_2/Si$ substrate.

europium concentration. The phase structure of ZrO_2 significantly influences its physical properties. Since all the thin films with different Eu contents show tetragonal phases without phase change, it is likely that the thin films have stable capacitance densities with a small variation of less than 0.5% within bias electric field of 500 kV/cm.

Fig. 6 exhibits the I–V characteristic of the $5\%Eu_2O_3$–$3\%Y_2O_3$–$92\%ZrO_2$ thin film deposited on $Pt/TiO_2/SiO_2/Si$ substrate. The leakage current density is about 6.5×10^{-7} A/cm^2 at 300 kV/cm. This lower leakage current can be attributed to the large energy band gap and Schottky barrier height of the YSZ thin films [17,18]. It has been suggested that Schottky electron emission is likely to be a significant source of leakage current in high-dielectric gate materials [18]. The larger Schottky barrier heights of YSZ thin films can provide a sufficiently large electron barrier against electron emission.

Fig. 7(a) shows the emission spectrum of the $5\%Eu_2O_3$–$3\%Y_2O_3$–$92\%ZrO_2$ thin film deposited on fused silica substrates annealed at 700 °C for 1 h in air. The photoluminescence photograph is shown in the inset of Fig. 7(a). Under 396 nm light excitation, the thin film deposited on fused silica substrate exhibits bright red photoluminescence with two emission peaks at 593 nm and 609 nm, which correspond to the $^5D_0\rightarrow{}^5F_1$ and $^5D_0\rightarrow{}^5F_2$ transitions of Eu^{3+} ions, respectively. Fig. 7(b) shows the excitation spectrum of the $5\%Eu_2O_3$–$3\%Y_2O_3$–$92\%ZrO_2$ thin film deposited on fused silica substrate annealed at 700 °C for 1 h in air. The excitation spectrum of the thin film was monitored at 609 nm. The peaks at 396 nm and 466 nm are due to $^7F_{0,1}\rightarrow{}^5L_6$, $^7F_{0,1}\rightarrow{}^5D_2$ transitions of Eu^{3+} ions, respectively. Additionally, a small shoulder is visible at around 255 nm. It is typical Eu^{3+} charge transfer excitation in the zirconia host [12].

We also studied the impact of Eu concentration on the emission of the $x\%Eu_2O_3$–$(8-x)\%Y_2O_3$–$92\%ZrO_2$ thin

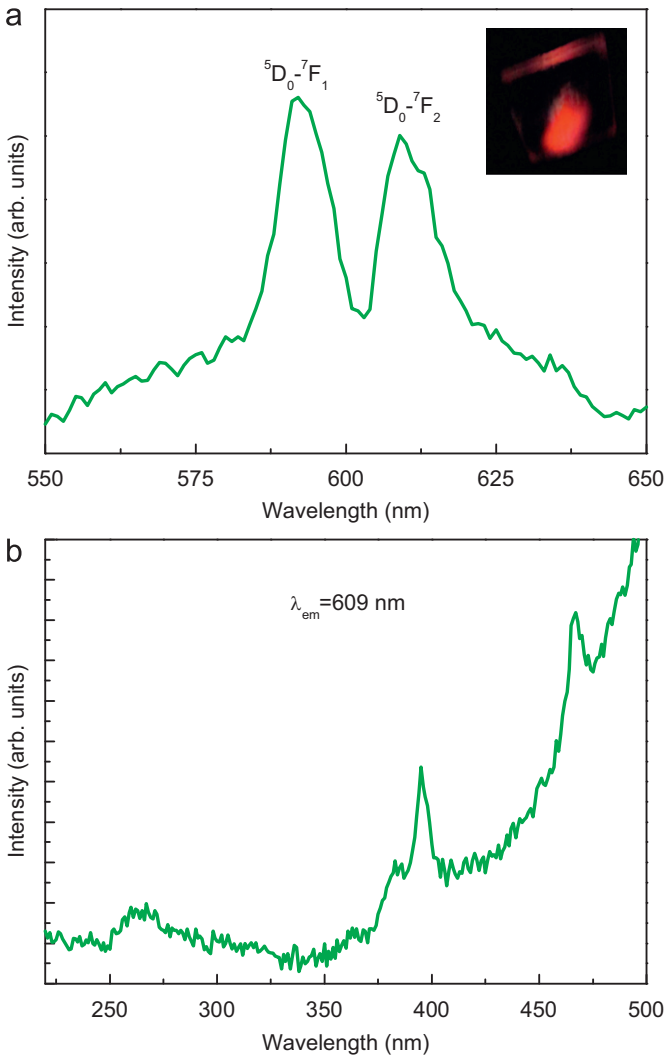

Fig. 7. (a) The emission and (b) excitation spectra of the $5\%Eu_2O_3$–$3\%Y_2O_3$–$92\%ZrO_2$ thin film deposited on fused silica substrate annealed at 700 °C for 1 h in air. The inset (a) shows the photoluminescence photograph of the thin film.

films ($x=0$, 1, 3, 5, and 7, respectively) deposited on $Pt/TiO_2/SiO_2/Si$ substrates. Fig. 8 shows the emission spectra of Y/Eu-codoped ZrO_2 thin films. The emission intensity gradually increases with increasing europium content and finally saturates. The $5\%Eu_2O_3$–$3\%Y_2O_3$–$92\%ZrO_2$ thin film shows the strongest emission. Previous luminescence studies of the Eu-doped ZrO_2 nanoparticles as a function of Eu^{3+} content carried out by Ninjbadgar and coworkers demonstrated that both the dopant concentration and the site symmetry of Eu^{3+} ions played an important role in the emission properties [12].

At the same time, the optical properties of the Y/Eu-codoped zirconia thin films were also studied from optical transmission spectrum in the wavelength range of 200–850 nm. Fig. 9 shows the optical transmission spectrum of the $5\%Eu_2O_3$–$3\%Y_2O_3$–$92\%ZrO_2$ thin film deposited on fused silica substrate annealed at 700 °C for 1 h in air. The thin film is highly transparent and colorless to the light with wavelength longer than 250 nm. The transmission drops rapidly at 250 nm, and the sharp absorption edge is at around 210 nm. The band gap energy is determined to be 5.5 eV for band gap transition of the thin film, which is close to the theoretical value of ZrO_2 (5.8 eV) [5].

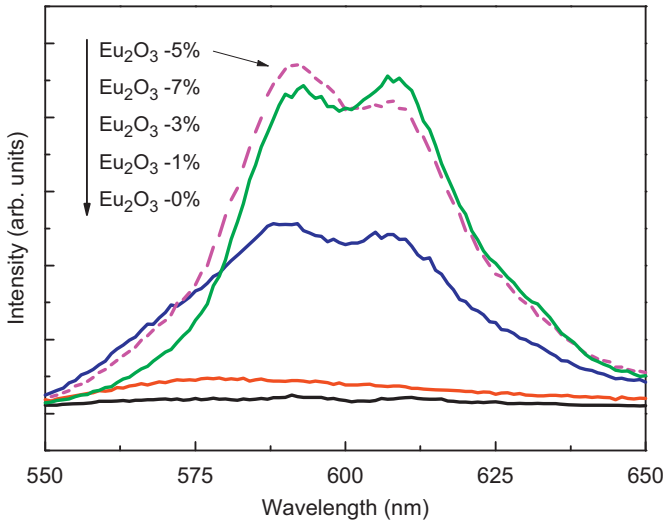

Fig. 8. The emission spectra of the $x\%Eu_2O_3$–$(8-x)\%Y_2O_3$–$92\%ZrO_2$ thin films ($x=0$, 1, 3, 5, and 7, respectively) prepared on $Pt/TiO_2/SiO_2/Si$ substrates.

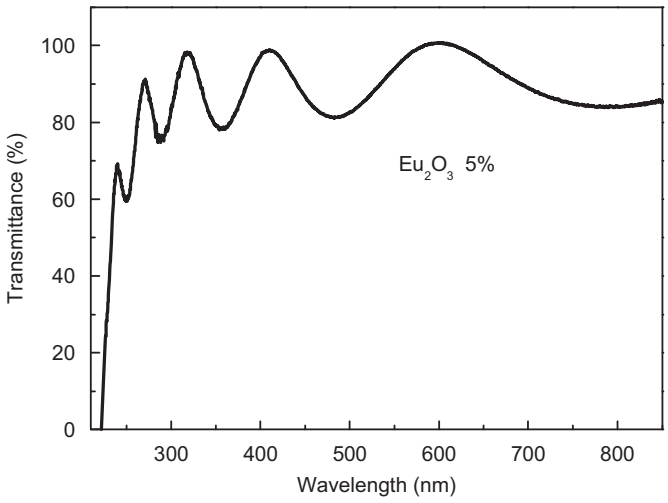

Fig. 9. The optical transmission spectrum of the $5\%Eu_2O_3$–$3\%Y_2O_3$–$92\%ZrO_2$ thin film deposited on fused silica substrate.

4. Conclusions

Y/Eu-codoped zirconia thin films have been prepared on fused silica and $Pt/TiO_2/SiO_2/Si$ substrates. The thin films simultaneously possess excellent photoluminescence and improved electrical properties, such as bright emission, reduced dissipation factor, and low leakage current density. Our results suggest that the Y/Eu-codoped zirconia thin films might have potential applications for new integrated optoelectronic and photonic devices.

Acknowledgments

The authors gratefully acknowledge financial support from the Natural Science Foundation of China (no. 51172289), the Natural Science Foundation of Guangdong Province, China (no. 10251027501000007), and the Specialized Research Fund for the Doctoral Program of Higher Education of China (no. 20110171130004).

References

[1] L. Liao, J.W. Bai, Y.C. Lin, Y.Q. Qu, Y. Huang, X.F. Duan, High-performance top-gated graphene-nanoribbon transistors using zirconium oxide nanowires as high-dielectric-constant gate dielectrics, Advanced Materials 22 (2010) 1941–1945.

[2] S.J. Wang, C.K. Ong, Epitaxial Y-stabilized ZrO_2 films on silicon: dynamic growth process and interface structure, Applied Physics Letters 80 (2002) 2541–2543.

[3] S.G. Wu, H.Y. Zhang, G.L. Tian, Z.L. Xia, H.D. Shao, Z.X. Fan, Y_2O_3 stabilized ZrO_2 thin films deposited by electron beam evaporation: structural, morphological characterization and laser induced damage threshold, Applied Surface Science 253 (2006) 1561–1565.

[4] C.Y. Lin, C.Y. Wu, C.Y. Wu, T.C. Lee, F.L. Yang, C.M. Hu, T.Y. Tseng, Effect of top electrode material on resistive switching properties of ZrO_2 film memory devices, IEEE Electron Device Letters 28 (2007) 366–368.

[5] C.L. Jiang, F.W. Nian, Q. Wu, X.G. Liu, Up- and down-conversion cubic zirconia and hafnia nanobelts, Advanced Materials 20 (2008) 4826–4829.

[6] J. Garcia-Barriocanal, A. Rivera-Calzada, M. Varela, Z. Sefrioui, E. Iborra, C. Leon, S.J. Pennycook, J. Santamaria, Colossal ionic conductivity at interfaces of epitaxial ZrO_2: $Y_2O_3/SrTiO_3$ heterostructures, Science 321 (2008) 676–680.

[7] J. Garcia-Barriocanal, A. Rivera-Calzada, M. Varela, Z. Sefrioui, E. Iborra, C. Leon, S.J. Pennycook, J. Santamaria, Response to comment on Colossal ionic conductivity at interfaces of epitaxial ZrO_2: $Y_2O_3/SrTiO_3$ heterostructures, Science 324 (2009) 465b.

[8] J.S. Lee, T. Matsubara, T. Sei, T. Tsuchiya, Preparation and properties of Y_2O_3-doped ZrO_2 thin films by the sol–gel process, Journal of Materials Science 32 (1997) 5249–5256.

[9] H. Zhou, X.M. Chen, G.H. Wu, F. Gao, N. Qin, D.H. Bao, Significantly enhanced red photoluminescence properties of nanocomposite films composed of a ferroelectric $Bi_{3.6}Eu_{0.4}Ti_3O_{12}$ matrix and highly *c*-axis-oriented ZnO nanorods on Si substrates prepared

by a hybrid chemical solution method, Journal of the American Chemical Society 132 (2010) 1790–1791.
[10] F. Gao, Q.Y. Zhang, G.J. Ding, N. Qin, D.H. Bao, Strong upconversion photoluminescence and large ferroelectric polarization in Er^{3+}–Yb^{3+}–W^{6+} triply substituted bismuth titanate thin films prepared by chemical solution deposition, Journal of the American Ceramic Society 94 (2011) 3867–3870.
[11] Y. Shen, D.R. Clarke, Effects of reducing atmosphere on the luminescence of Eu^{3+}-doped yttria-stabilized zirconia sensor layers in thermal barrier coatings, Journal of the American Ceramic Society 92 (2009) 125–129.
[12] T. Ninjbadgar, G. Garnweitner, A. Borger, L.M. Goldenberg, O.V. Sakhno, J. Stumpe, Synthesis of luminescent ZrO_2: Eu^{3+} nanoparticles and their holographic sub-micrometer patterning in polymer composites, Advanced Functional Materials 19 (2009) 1819–1825.
[13] H. Hobbs, S. Briddon, E. Lester, The synthesis and fluorescent properties of nanoparticulate ZrO_2 doped with Eu using continuous hydrothermal synthesis, Green Chemistry 11 (2009) 484–491.
[14] C.M. Perkins, B.B. Triplett, P.C. McIntyre, K.C. Saraswat, S. Haukka, M. Tuominen, Electrical and materials properties of ZrO_2 gate dielectrics grown by atomic layer chemical vapor deposition, Applied Physics Letters 78 (2001) 2357–2359.
[15] Y.C. Yeo, T.J. King, C.M. Hu, Metal-dielectric band alignment and its implications for metal gate complementary metal-oxide-semiconductor technology, Journal of Applied Physics 92 (2002) 7266–7271.
[16] J. Zhu, Z.G. Liu, Dielectric properties of YSZ high-k thin films fabricated at low temperature by pulsed laser deposition, Materials Letters 57 (2003) 4297–4301.
[17] S.J. Wang, C.K. Ong, S.Y. Xu, Electrical properties of crystalline YSZ films on silicon as alternative gate dielectrics, Semiconductor Science and Technology 16 (2001) L13–L16.
[18] J. Robertson, Band offsets of wide-band-gap oxides and implications for future electronic devices, Journal of Vacuum Science and Technology B 18 (2000) 1785–1792.